Spatiotemporal dynamics during niche remodeling by super-colonizing microbiota in the mammalian gut

Guillaume Urtecho[1], Thomas Moody[1,2], Yiming Huang[1,2], Ravi U. Sheth[1,2,3], Miles Richardson[1,2], Opeyemi Lekan[1,4], Florencia Velez-Cortes[1,2], Deirdre Ricaurte[1,2], & Harris H. Wang[1,5,#]

[1] Department of Systems Biology, Columbia University, New York, NY, USA.

[2] Integrated Program in Cellular, Molecular, and Biomedical Studies, Columbia University, New York, NY, USA

[3] Kingdom Supercultures, Brooklyn, NY, 11205

[4] Columbia College, Columbia University, New York, NY 10027

[5] Department of Pathology and Cell Biology, Columbia University, New York, NY, USA.

[#] Correspondences should be addressed to hw2429@cumc.columbia.edu.

ABSTRACT

Gastrointestinal colonization by commensal bacteria is a reproducible yet complex process. Mapping the spatiotemporal and genetic factors driving microbial colonization of the gut is key to understanding the gut microbiome and improving clinical interventions that treat dysbiosis. Here, we explored a murine gut colonization model that leveraged the natural inter-individual variations in gut microbiomes to elucidate the spatiotemporal dynamics of fecal microbiota transplantation (FMT). We identified a natural 'super-donor' consortium that universally engrafts into diverse recipients and resists reciprocal colonization. Upon FMT, the super-donor microbiota displaces a significant fraction of the recipient microbiome and stably persists over months. Metagenomic sequencing of this consortium revealed diverse metabolic genes that could participate in nutrient niche expansion. Temporal profiling of the gut microbiome showed an ordered succession of rapid engraftment by early colonizers within 72 hours followed by a slower emergence of late colonizers over 15-30 days. Moreover, microbial engraftment was localized to specific compartments of the gastrointestinal tract in a species-specific manner. Spatial metagenomic characterization and functional studies suggested that stable engraftment was mediated by simultaneous transfer of spatially co-localizing species from the super-donor consortia, many of which belonged to the *Bacteroidales* order. These results offer a mechanism of super-donor colonization by which nutritional niches are expanded in a spatiotemporally-mediated manner to promote successful engraftment into a resident gut microbiome.

INTRODUCTION

The mammalian gut microbiome is composed of hundreds to thousands of bacterial species that co-exist symbiotically with their host and provide key metabolic and protective functions[1–3]. Despite being subjected to the harsh gastrointestinal (GI) environment and experiencing constant washout and nutritional shifts, the gut microbiome develops reproducibly across people during early development and eventually reaches a steady state by adulthood[4]. Various environmental factors such as exposure to xenobiotics, antibiotics, or diet can lead to altered microbiome compositions and increased susceptibility to colonization of pathogens and pathobionts[5]. The recent success of fecal microbiota transplantation (FMT) to treat a disturbed gut microbiome suggests a robust process by which a healthy microbiome can be restored[6]. However, the detailed dynamics, mechanisms, and principles by which microbes successfully engraft into a resident community remain unclear.

The stability and malleability of a microbiome is shaped by various ecological properties including networks of inter-microbial interactions that manifest spatially and dynamically over time[[7–9]. Metabolic interactions arise from commensal or mutualistic degradation of complex substrates that support multiple species in a consortium[10,11]. In the gut, *Bacteroides* are known to excrete various carbohydrate degradation enzymes that in concert liberate various sugars for dietary polysaccharide[10]. Similarly, diverse microbes spanning the length of the gut participate in the deconjugation and step-wise biotransformation of host-secreted bile acids, which alters local biochemical environments resulting in dramatic effects on gut biogeography[12]. Often, these metabolic activities reinforce positive-feedback loops that gradually result in systemic changes to the gut environment over sustained periods of time[13,14,15]. Mapping these interspecies interactions are key for assessing the stability of the microbiome and its susceptibility to colonization by other microbes.

The ability to colonize and shape microbial communities by introducing foreign microbiota is a quintessential goal of FMT therapies. Despite many successes, these therapies have exhibited mixed outcomes that vary between different combinations of donors and recipients. Curiously, “Super donors” that consistently engraft in a variety of recipients have been reported[16]. While this phenomenon has been generally linked to the species richness and diversity of donor communities, it is currently unclear what specific mechanisms or determinants are responsible[17,18]. The maturation of these therapies is thus reliant on developing an understanding of several key questions: Why do some strains engraft when others do not? Is variability in engraftment success due to donor or recipient composition or are there other factors? As the composition of these microbial communities change, does their spatial structure change to

resemble the donor? To answer these questions, we need effective models for studying variable FMT outcomes and tools to dissect the microbial spatiotemporal dynamics and ecological interactions occurring *in vivo*.

In this work, we use a murine model system that exploits natural variation in gut microbiomes to study the temporal and spatial dynamics of microbial engraftment during FMT. This model recapitulates some of the key features of human FMT including recipient heterogeneity, temporal components, & diet dependency while also giving us total control of the experimental parameters in contrast to human FMT trials. We show that microbiomes of C57BL/6 mice acquired from different vendors exhibit variable outcomes when subject to pairwise FMT and identify a "Super Donor" consortium. We find that transplantation and successful engraftment of microbes by this consortium occurs over short and long-term emergence events characterized by distinct microbial taxa. Furthermore, we examine the spatial distribution of microbial engraftment across the recipient gastrointestinal tract and identify key genetic factors associated with engraftment across different areas of the murine GI tract. Finally, we use Metagenomic plot sampling by sequencing (MaPS-Seq) to study how the micron-scale spatial structure of microbial communities are affected by engraftment and demonstrate that these changes modulate the metabolic capacities of the FMT recipient microbiome. These results introduce a conceptual mechanism wherein colonizing microbes remodel metabolic niches within gut environments to facilitate microbial colonization.

RESULTS

A natural murine model of gut microbiome variability and diversity

To determine whether murine FMT models could be a suitable surrogate for human studies, we first explored whether the murine gut microbiome exhibited the same degree of intra-host variability that is commonly observed in human populations[15,19]. Previous studies suggested that genetically identical mice sourced from different suppliers had distinct gut microbiota[20–22]. To verify these findings, we obtained conventional C57BL/6 mice from four different commercial suppliers (Jackson Labs, J; Taconic, T; Charles River, C; and Envigo, E) and performed 16S sequencing on their fecal matter (**Fig 1A**). Indeed, we observed that the gut microbiome from different suppliers had consistently distinct compositions in terms of taxa or OTUs (Operational Taxonomic Units) present and substantial differences in alpha diversity (**Figure 1B, 1C**). Mice from Envigo displayed the greatest diversity, marked by high levels of *Prevotellaceae* and *Muribaculaceae*, while Jackson Labs mice had the lowest diversity with an elevated proportion of *Firmicutes* relative to *Bacteroides* (**Figure S1A**). In humans, an increase in *Firmicutes*-to-

Bacteroides ratio has been linked to obesity and IBS[23–25]. Importantly, the difference in microbiome diversity between mice cohorts is around the same degree as between healthy human cohorts and those with gastrointestinal disorders[26,27] (**Figure S1B**). Therefore, the inter-vendor variability of the murine gut microbiome may be a tractable surrogate model for studying the principles guiding microbiota transfer between natural assemblages, which could help reveal shared properties underlying human FMT engraftment and outcomes.

Beyond taxonomic composition, functional diversity within the metagenome is a key driver of community assemblage. To catalog the functional diversity across mice gut microbiomes from different suppliers, we performed shotgun metagenomic sequencing on their fecal DNA, which yielded a 240 Gb dataset that assembled into 457 metagenome-assembled genomes (MAGs) with annotated gene functions (Methods). This collection of MAGs covered over 80% of all genus-level diversity across the four distinct C57BL/6 gut microbiomes and is to our knowledge the most comprehensive of its kind for mice (**Fig 1D**). Upon taxonomically assigning MAGs, we found that Envigo consortia harbored a distinctly higher diversity of *Muribaculaceae*, which are known to be prolific mucin foragers with diverse polysaccharide degradative capacities[27]. More detailed genomic characterization of the Carbohydrate-Active Enzyme (CAZyme) repertoire within *Muribaculaceae* MAGs revealed that the Envigo microbiome contained the highest number of glycoside hydrolase (GH) genes, especially those involved in the breakdown of glucans and glycosides (**Figure 1E**). Furthermore, *Muribaculaceae* MAGs from Envigo contained a set of unique CAZymes, which may indicate these bacteria are able to utilize a broader range of dietary polysaccharides (**Figure 1F**). Beyond CAZyme differences, we did not find any other KEGG pathway enrichments amongst the MAGs (**Figure S1C**). These findings highlight that the mouse gut microbiomes derived from different vendors exhibit unique compositional and functional variations to a similar degree as that found in human populations.

Variable engraftment of gut microbiota in a murine model of FMT

The inter-vendor variability in murine gut microbiomes is a useful property for an experimental model of microbial gut colonization that mimics the process of FMT[2829]. We therefore aimed to implement a simple, yet robust protocol that does not require pre-conditioning of the microbiome (e.g., use of antibiotics), and can leverage the natural variations in gut microbiomes of otherwise genetically identical mice. It is well established that cohoused mice from the same cage have near identical gut microbiomes because of fecal-oral transmission via coprophagy[[28,30]. Leveraging this behavior, we cohoused mice from four different suppliers in a pairwise manner and profiled their gut microbiota by fecal 16S sequencing before cohousing (Day 0) and after five

days (Day 5) (**Figure 2A**). Interestingly, we observed variable outcomes in terms of the number of OTUs transferred between different pairs of mice (**Figure 2B**). In most cases, bi-directional transfer of taxa occurred between different mice, with the number of unique OTUs transferred scaling accordingly with the microbiota diversity present in the donor. Members of the Envigo microbiome, which exhibited the greatest diversity, were capable of engraftment into all other microbiota and were highly resistant to reciprocal colonization. A group of 20-30 Envigo "super-donor" OTUs effectively transfers to all different recipient microbiota, suggesting a robust but complex ecological process underlying the observed colonization rather than random outcomes as predicted by the neutral theory of community assemblages[31,32]. Transferred microbes from Envigo donors were generally of the *Muribaculaceae* family but also included other taxa, including *Bacteroidaceae* and *Prevotellaceae spp.* (**Figure 2C**). In addition to acquisition of new taxa, several OTUs initially present in the recipients were displaced after exposure to the Envigo microbiota (**Figure S2A**). For instance, in Jackson and Charles River recipients *Muribaculaceae spp.* were mainly displaced by Envigo *Muribaculaceae*. Therefore, Envigo microbiota appear to exhibit a super-donor phenotype that is sometime observed in human FMT trials[[33]. Recalcitrance of Envigo microbiota to invasion or displacement by other microbiota highlights this dominant persistence and colonization resistance phenotype.

Ordered temporal microbiota transfer during murine FMT

To better elucidate the temporal dynamics of microbial transfer during our FMT model, we performed fecal 16S profiling of Jackson (Jax) mice cohoused with Envigo (Env) mice over 32 days. We observed dramatic changes to the microbiomes of Jax mice cohoused with Env mice (Env2Jax) at both short (days) and long (weeks) time scales associated with the emergence or displacement of particular OTUs (**Figure 3A**). Microbes transferred from Env to the Jax gut within the first five days were mostly *Lactobacillaceae* and *Muribaculaceae* whereas *Lachnospiraceae* emerged and reached high relative abundance over the latter half of this time-course experiment (**Figure 3B**). Overall, 33 unique OTUs engrafted into Env2Jax mice, with 21 (63.4%) of these transferring within the first five days of cohousing (**Figure 3C**). At the conclusion of this time course, the Env2Jax microbiome exhibited higher population diversity and clustered more closely with the Env microbiome based on principal component analysis (PCA) (**Figure S3A, S3B**). As a control, cohoused cage mates from the same vendor did not lead to notable changes in the gut microbiome for both Env and Jax mice (**Figure S3C, Figure S3D**). We therefore conclude that most taxa engraft quickly after initial FMT, but some taxa emerge over a longer period, which may indicate a gradual transition in the gut milieu towards stabilization.

Engraftment of new OTUs may correspond to expansion of niches reflected by an increase in carrying capacity of the community. We therefore assessed changes in bacterial density throughout FMT using absolute abundance measurements of fecal samples (Methods). Despite the consistent increase in unique OTUs observed over time, overall population load exhibited substantial temporal fluctuations. Overall biomass decreased over the first two days before a dramatic expansion followed by an equilibration (**Figure 3D**). By Day 30 the relative biomass corresponding to taxa specific to the Jax microbiota was entirely replaced by Env taxa. While Env mice cohoused with Jax mice also experienced a population-level bottleneck at Day 2 there was no dramatic increase in biomass and the microbiome ultimately reverted back to its original state. Neither control groups showed this phenomenon (**Figure S3E**). Our data therefore suggests that the convergence of microbial communities during FMT results from a transitionary state with a rapid and dramatic interval of population bottlenecking, followed by restructuring and re-equilibration of the new community.

Microbial transplantation dynamics vary across murine gut compartments

The mammalian gut contains many ecological niches whose diverse environmental, biochemical, and ecological properties shape the gut biogeography, resulting in distinct microbial populations across different gut compartments[34]. Therefore, analysis of fecal pellets gives an incomplete picture of all changes occurring along the intestinal tract since fecal matter predominantly reflects the distal gut [[35–37]. To explored engraftment dynamics across different compartments along the murine intestinal tract following FMT, we obtained GI samples upon necropsy at the conclusion of the 32-day Env-Jax cohousing experiment and performed 16S and metagenomic profiling of individual gut compartments spanning the entire intestinal tract (**Figure 4A**). We observed that the 16S microbiome profiles of Env2Jax mice at Day 32 resembled the Env microbiome across all gut compartments with distinct populations occupying each gut compartment. Interestingly, the taxonomic composition of the Jax microbiome appeared to be more uniform across gut compartments. In contrast, the gut microbiome of Env and Env2Jax cohorts were more stratified, with distinct microbial profiles in the small and large intestines. In addition, the spatial distribution of many OTUs already found in Jax mice changed across the gut (**Figure 4B**). This shows that microbial transfer by FMT results in non-uniform colonization across different areas of the gut and alters the biogeography of native species.

To quantitatively assess how overall microbial communities were affected across different sections of the GI tract, we looked at changes in the biomass of different taxonomic groups in these areas. The composition of engrafting microbes varied dramatically across different

compartments. *Lactobacillaceae* were the primary colonizers of the small intestines, whereas diverse populations including *Muribaculaceae, Prevotellaceae, and Lactobacillaceae* colonized the cecum and colon of Env2Jax mice (**Figure 4C**). Conversely, a majority of the recipient-specific biomass was displaced, especially within upper-GI compartments where overall bacterial biomass decreased by as much as 97.2% in the duodenum (**Figure 4D**). As was observed in our longitudinal profiling, OTUs specific to the Jax microbiome were nearly entirely replaced across all gut compartments while a proportion of the microbial taxa shared between the Env donor and Env2Jax decreased from 85-70% to 15-30% of the population of each gut compartment (**Figure 4E**). These data reflect the highly variable effects of FMT on microbial biomass and composition between intestinal compartments in the recipient.

Next, we explored whether the timing of 'early' or 'late' colonizing species was related to the areas they colonized in the gut. We compared the distribution of microbes to the order they colonized the GI tract observed in our longitudinal study (**Figure S4A**). Interestingly, "early colonizing" bacteria (mainly *Lactobacillaceae*) were more commonly observed in the upper GI whereas "late colonizers" were relatively enriched in the cecum and colon. Late-colonizing species nearly exclusively consisted of *Lachnospiraceae*, the abundance of which are positively correlated with microbial production of deoxycholic acid (DCA)[38]. Considering conversion of primary bile acids to DCA is predominately facilitated by microbes in the upper GI[39], early colonizing microbes may gradually alter DCA levels, enabling colonization by *Lachnospiraceae*. This raises the possibility that the late colonization phenomenon is due to early colonizers changing the biochemical properties of the gut before conditions are permissive to late colonizers.

FMT results in restructuring of micron-scale species co-associations

The murine gut microbiome exhibits local spatial structuring that reflects complex inter-microbial interactions driven by various mutualistic, commensal, and competitive processes[40]. Given the dramatic changes to the microbiome of Jax recipients upon FMT, we sought to characterize the changes to the spatial structure of the Jax microbiome using MaPS-seq, a sequencing-based method recently developed in our lab to obtain micron-scale species co-association information from the gut microbiome[40,41]. We used fecal matter for these analyses since they largely reflect spatial structuring of colonic microbiota.

Using MaPS-seq, we characterized the spatial arrangement of microbes in fecal communities from Env2Jax and compared the microbial spatial co-associations to the those found in the Env donor as well as the Jax control. After quality filtering, we recovered the 16S profiles of 89,170 MaPS-seq particles, which clustered into 27 distinct spatially co-associated sub-

communities (**Figure 5A**). These clusters contained between 4 and 37 distinct OTUs and varied dramatically in their taxonomic composition even at the class-level (**Figure S5A**). Particles derived from Env2Jax mice generally clustered with Env donor-derived particles, although some clusters contained particles from all mouse groups (**Figure S5B**). Overall, we observed a variety of changes in the proportion of each cluster found in Env2Jax compared to Jax mice (**Figure 5B**). Jax community clusters enriched in Clostridia species were severely depleted following FMT while *Bacteroidia*-enriched clusters grew in abundance. This suggests a community-wide shift in the key ecological species within these communities from a *Clostridia*-centric ecosystem towards one structured around *Bacteroidia*.

Next, we investigated the change in ecological interaction following FMT by inferring significant spatial co-associations between microbes across MaPS-seq particles. We implemented an empirical Bayesian approach to identify microbes co-occurring within particles at frequencies significantly greater or less expected frequencies[42]. Microbes co-occurring at frequencies greater than expected by chance are presumed to engage in positive interactions (e.g., commensalism or mutualism) whereas microbes co-occurring at reduced frequencies are presumed to engage in negative interactions such as competitive exclusion or antagonism. We identified 333 significant interactions in the Jax microbiome prior to FMT whereas only 220 were identified in Env2Jax microbiomes. In both cases, positive interactions were more common than negative interactions. Interestingly, an overwhelming majority interactions in Jax microbiota were predominately found between shared OTUs present in both the Jax and Env communities, whereas OTUs unique to Jax microbiome were involved in far fewer interactions (**Figure S6**). Conversely, microbes unique to the Env microbiome exhibited many interactions amongst themselves as well as with this shared microbiome. This indicates that microbes unique to the Env microbiome form spatially-associated units whereas microbes unique to the Jax recipient are spatially isolated.

To observe changes to the overall interaction landscape of these communities, we performed a network analysis of significant interactions (**Figure 5C**). In Jax communities, two OTUs, members of the class *Bacilli* and *Clostridia*, were the most prolific interactors. In Env2Jax communities, there was a large shift in the interaction landscape, wherein many OTUs of the class *Bacteroidia* form interconnected spatial-association networks, indicative of a community unit brought together by mutualistic or commensal interactions. To look at overall changes, we determined the number of positive and negative interactions occurring between taxonomic groups in Jax and Env2Jax FMT communities (**Figure 5D**). In Jax communities, a majority of positive and negative interactions were observed between *Clostridia* and a handful of interactions appeared

with other obscure members of the microbiome. In contrast, in Env2Jax communities we observed a large shift in the interaction landscape, towards almost exclusively amongst *Bacteroidia* which were overwhelmingly positive. This indicates that FMT resulted in large-scale ecological and spatial remodeling of the gut microbiome, which may potentially coincide with altered behaviors of these communities in the gut environment.

Lastly, we explored whether these spatial associations were predictive of FMT outcomes for donor microbes. Indeed, we found donor microbes with greater than 2-fold enrichment in Env2Jax mice relative to Jax mice exhibited significantly more spatial associations than microbes that were not enriched or depleted (**Figure 5E**). These results suggest that microbes that transfer as spatially-associating units are better able to engraft than spatially isolated species.

Exploitation of open nutritional niches as a key determinant of FMT engraftment success

Given that Env microbiota contained spatially-associating *Bacteroidia* communities that participated in cooperative interactions, we sought to explore how Jax and Env *Bacteroidia* communities differed in their metabolic capacities to access nutrient niches in the gut environment. *Bacteroidia* are the primary metabolizers of complex dietary polysaccharides in the gut and work in concert to breakdown these macromolecules into consumable subunits [[10]. Interestingly, gut colonization of engineered probiotics can be enhanced by fiber supplementation, in cases where the probiotic is the sole species capable of metabolizing that fiber[43,44]. Therefore, we hypothesized that the super-colonizing phenotype of Env *Bacteroidia* is driven by their ability to metabolize previously inaccessible dietary fibers within the Jax recipient GI tract. We evaluated the abilities of fecal communities from Env, Env2Jax, and Jax mice to utilize various complex polysaccharides. We performed growth assays on their fecal communities over 48 hours using defined minimal media supplemented with a panel of complex carbohydrates to characterize the range of polysaccharides accessible to each community. In this format, growth would only be possible if these microbial communities were able to break down the supplemented complex polysaccharides. We observed striking differences in growth profiles, where the Envigo donor and Env2Jax fecal populations exhibit broad capacities to utilize complex dietary polysaccharides that were unusable by the control Jax microbiota (**Figure 5F**). Interestingly, the native Jax communities grew faster in glucose, arabinan, and arabinogalactan indicating a population specialized for using these resources. 16S profiling of saturated communities showed that more diverse populations grew from the Env and Env2Jax fecal communities in all conditions (**Figure S7**). This is the consistent with the hypothesis that mixed communities of engrafted *Bacteroidia* work cooperatively to break down previously unused dietary polysaccharides into available

carbohydrates. We conclude that the Env fecal communities can access a broader set of carbohydrate nutrients to supplement their growth allowing them to exploit unfilled nutrient niches in the recipient gut. FMT from these communities imparts the ability for this ecosystem to metabolize additional carbohydrates, which may expand available nutrient niches within the recipient gut.

Using humanized mouse gut microbiomes to simulate human FMT outcomes

Finally, we explored the use of our murine model to simulate FMT dynamics between humans. We acquired fecal samples from three representative human donors of the three major human gut microbiome enterotypes[45]. These individuals, H1, H3, and H5, were dominated by *Ruminococcae* (enterotype 3), *Prevotellaceae* (enterotype 2), and *Bacteroidaceae* (enterotype 1), respectively. We gavaged germ-free mice with these fecal samples and observed the successful engraftment after nine days, with varying degree of diversity (**Figure S8A**). Humanized mice were predominately colonized by families *Bacteroidaceae* and *Akkermansiaceae* regardless of the enterotype of the donor, whereas *Prevotellaceae* and *Ruminococcaceae* were poorly represented, which has been previously noted[cite]. Furthermore, the microbiomes of humanized mice were similar at the family-level but varied greatly when comparing OTU-level resolution and diversity metrics, where the H5 mice displayed the highest diversity (**Figure S8B**). Although humanized mice microbiomes did not fully recapitulate the microbiomes of their donors[46], PCA analysis showed the greatest similarity to their respective donors (**Figure S8C**). Ultimately, we find that mice are best able to recapitulate the microbiomes of *Bacteroidaceae*-enriched human gut microbiomes following humanization by FMT.

Next, we performed pairwise co-housing between these mice to determine whether humanized mice could be used to explore FMT outcomes between human microbiomes (**Figure 6A**). After nine days of cohousing, fecal 16S sequencing identified three main clusters of microbes that were transferred between these humanized mice microbiomes and were generally enriched for members of the order *Clostridiales* **(Figure 6B)**. While microbes generally transferred to both or neither recipient, Cluster 3 transferred from H3 to H5 but did not transfer from H3 to H1, indicating incompatibility with this group and the H1 microbiome. Interestingly, we did not observe any notable clusters where the *Bacteroidales*-enriched H5 microbes transferred to either recipient despite this cohort exhibiting the highest diversity. Overall, we found that humanized murine models are amenable to studying FMT outcomes between consortia of human microbiota.

DISCUSSION

Our results demonstrate several key features of microbial colonization in a murine model following FMT. Firstly, we describe how these populations are established over time and note that the process of establishing populations occurs over long periods overtime characterized by multiple surges of distinct microbial taxa. We hypothesize that following initial colonization events, newly established microbes begin a gradual process of shaping the gut environment which ultimately paves the way for other transferred species to gain foothold. Future studies should examine the metabolic and biochemical changes that occur during this process, which may reveal new facets about how microbial communities interact and are established. A particularly interesting observation from this temporal analysis was the sharp drop in overall microbial population size in the short-term following FMT followed by a bloom and subsequent stabilization. This observation may be explained by the results of a previous longitudinal study, which showed that dramatic population transitions exhibit an initial population-level bottleneck before dense, stable communities are established[47]. This may be a general phenomenon that occurs during the merging of microbial communities and warrants further investigation to learn the microbial dynamics and interactions controlling this process.

Secondly, our analysis of engrafted communities across the GI tract provided the opportunity to explore how colonization mechanisms differ across these areas. Considering the variance in biogeography across the GI tract, it is not surprising that microbial colonization following FMT would vary to a commensurate degree. While we find that certain microbial activities such as carbohydrate utilization and bile acid hydrolysis are associated with colonization in different gut compartments, future work should explore in greater detail the roles and mechanisms of these colonization factors in microbial fitness and interactions. The ability to harness these colonization factors to improve engraftment of probiotic therapeutics and predict FMT outcomes would empower these therapies and enable personalized approaches.

Considering microbial communities in the upper GI can alter downstream conditions such as bile acid profiles and SCFA content, FMT-induced changes to microbial communities in the small intestines likely affect microbial colonization in the lower GI. This may hint at a potential explanation for the appearance of microbes over multiple time scales following FMT, in which the early colonizers of the small intestines, over time, alter downstream gut environments until they are suitable for secondary colonizers. In our study, *Lactobacillae spp.* constituted an appreciable proportion of early colonizers and were primarily found within the small intestines. Given that these are major players in shaping bile acid content within the gut[48], it is possible that the introduction of these new *Lactobacillae* affected bile acid processing by the microbiome thereby

altering secondary bile acid pools in the lower GI. To this point, the late colonizers we observed were mostly comprised of *Lachnospiraceae* whose abundances in the murine intestines have been shown to positively correlate with secondary bile acid levels[49]. Further studies should consider these 'long-distance' interactions of the microbiome and their consequences on microbial engraftment by microbial consortia.

Lastly, we used MaPS-seq[cite] to explore changes in the spatial structure of microbial communities after FMT, showing for the first time the micron-scale consequences of FMT on communities within the recipient gut. This analysis led us to the interesting observation that microbes within spatially-associated communities were best able to successfully colonize and persist in recipient GI tract. In our test case, these spatially associated communities were able to expand the capacity of the recipient microbiome to metabolize diverse polysaccharides. We were particularly interested by a transferred community enriched with members of the order *Bacteroidales*, which led us to observe that communities transferred from Envigo donors are capable of broadly utilizing polysaccharides inaccessible to the Jackson recipient microbiomes, which grew faster but only in a limited range of carbohydrates. We believe the trade-off of generalist vs specialist communities may be an important factor in determining the success of FMT therapies and that generalists communities may be better suited for engraftment into recipients. Given that the mammalian intestinal tract is a dynamic environment, with constantly fluctuating available resources and host-derived inputs[5051], generalists may be more effective at enduring these changing conditions and supplanting populations of specialists. Indeed, similar observations have been made during the merging of aquatic microbial communities exhibiting dynamic environmental conditions[52]. Another explanation for the success of generalist communities is that the broad range of nutrients they can utilize equips them to exploit unused nutritional niches within recipient gut environments. The creation of nutritional niches has shown to be an effective tool for enabling engraftment of probiotic microbes[43,53], yet we show here that niche exploitation may be possible independent of dietary supplements to facilitate transplantation of microbial communities in the mammalian GI tract.

In this work we systematically explored the spatiotemporal dynamics of microbial colonization following FMT. We used a murine system for performing FMT between diverse, healthy gut communities that yields variable outcomes depending on recipient-donor combinations. In addition, we show this system is amenable to performing FMT between mice with "humanized" gut microbiomes. While this system misrepresents host-associated factors that differ between murine and human gastrointestinal tracts, we expect it will be a valuable resource

for studying inter-microbial interactions that play significant roles in shaping resultant population structures from FMT.

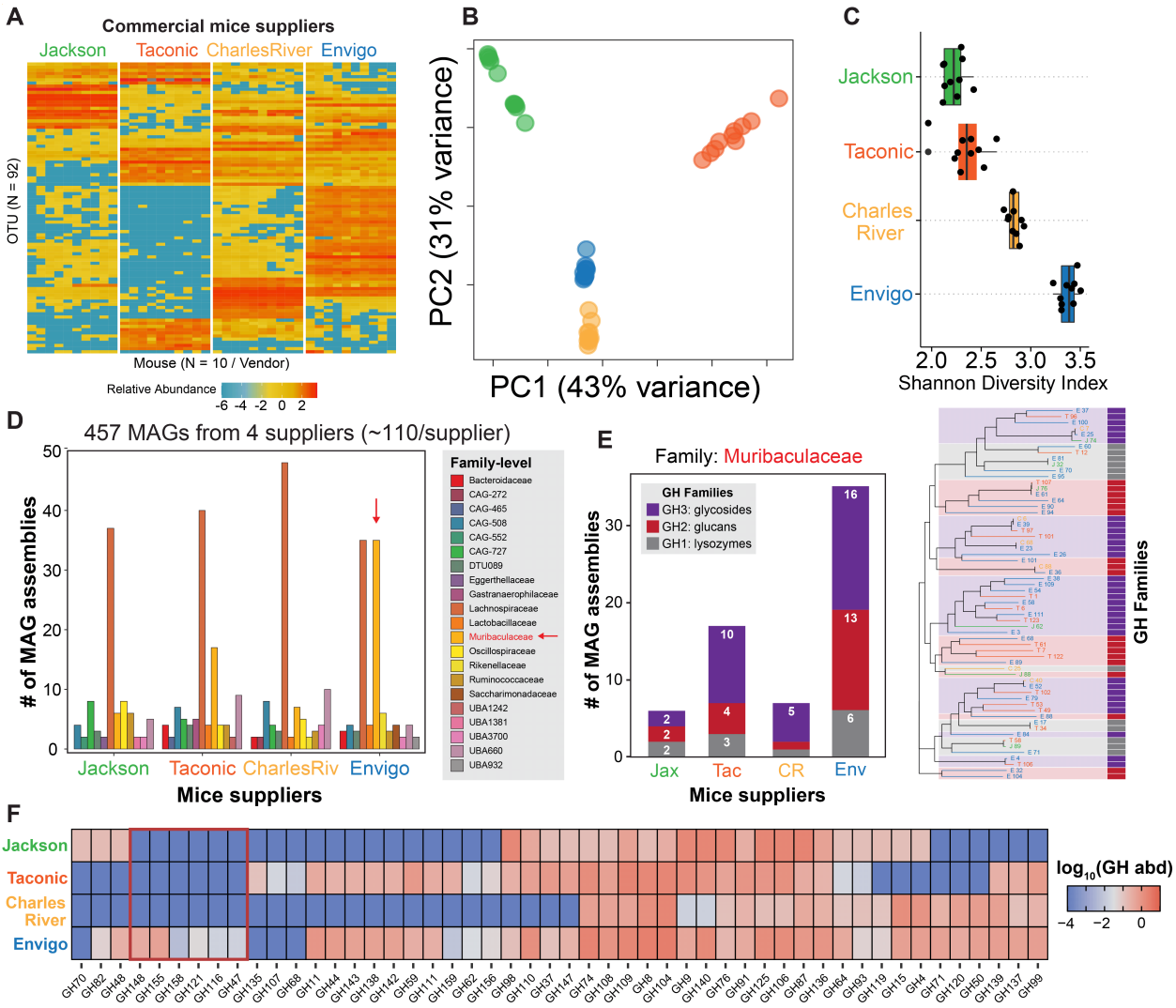

Figure 1. Microbiome profiles of C57BL6/J mice are distinct between suppliers. **(A)** Microbiome composition of BL57BL/6 mice sourced from four vendors by 16S rRNA sequencing (N = 10 mice / vendor). **(B)** PCA of microbiome composition between mouse cohorts using euclidean distance. **(C)** Shannon diversity index of mouse microbiomes. **(D)** Number of metagenome-assembled genomes (MAGs) associated with each vendor and their family-level taxonomic distribution. **(E)** (left) Number of MAGs within each microbiome containing genes corresponding to glycoside hydrolase (GH) families 1-3. (right) Phylogenetic analysis of GH family 1-3 genes identified in MAGs. **(F)** Abundance of glycoside hydrolase genes within *Muribaculaceae* MAGs from each vendor.

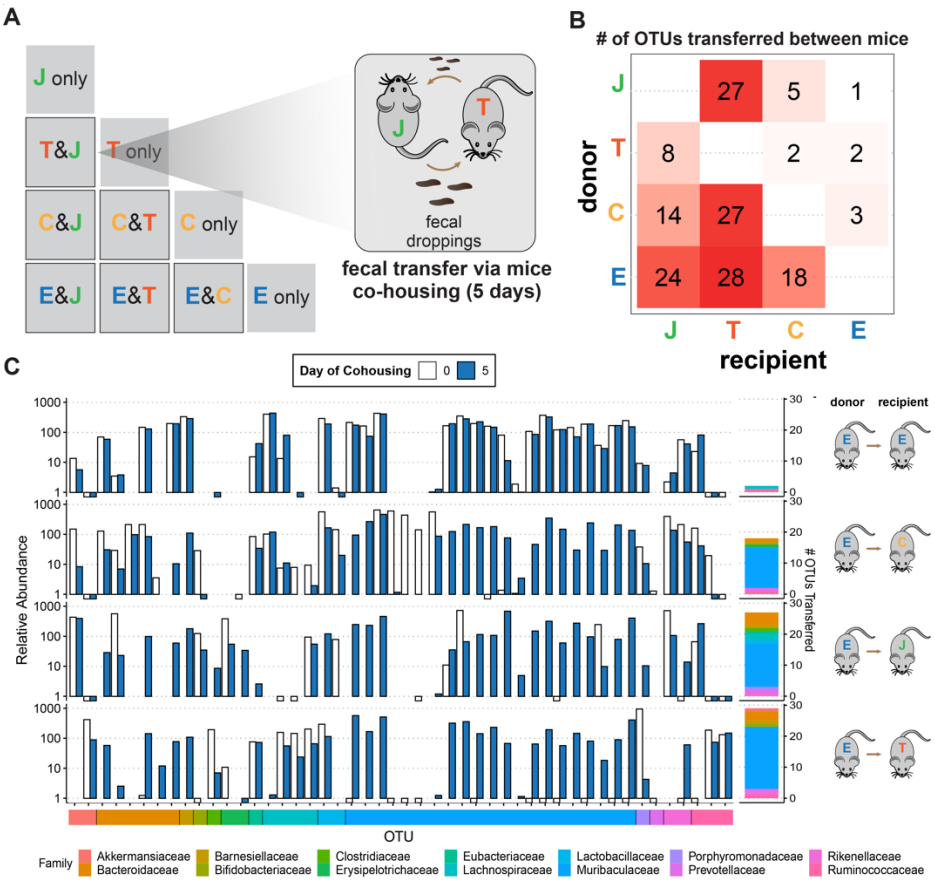

Figure 2. Diverse murine gut microbiomes exhibit variable outcomes to pairwise FMT. **(A)** Pairwise fecal microbiota (FMT) transfer model by co-housing female BL57BL/6 mice from different vendors. **(B)** Number of OTUs transferred between pairs of mice. **(C)** (left) Relative abundance of OTUs at Day 0 and Day 5 of cohousing with mice acquired from Envigo. (right) Number and taxonomic identity of OTUs transferred from Envigo microbiome to various recipient.

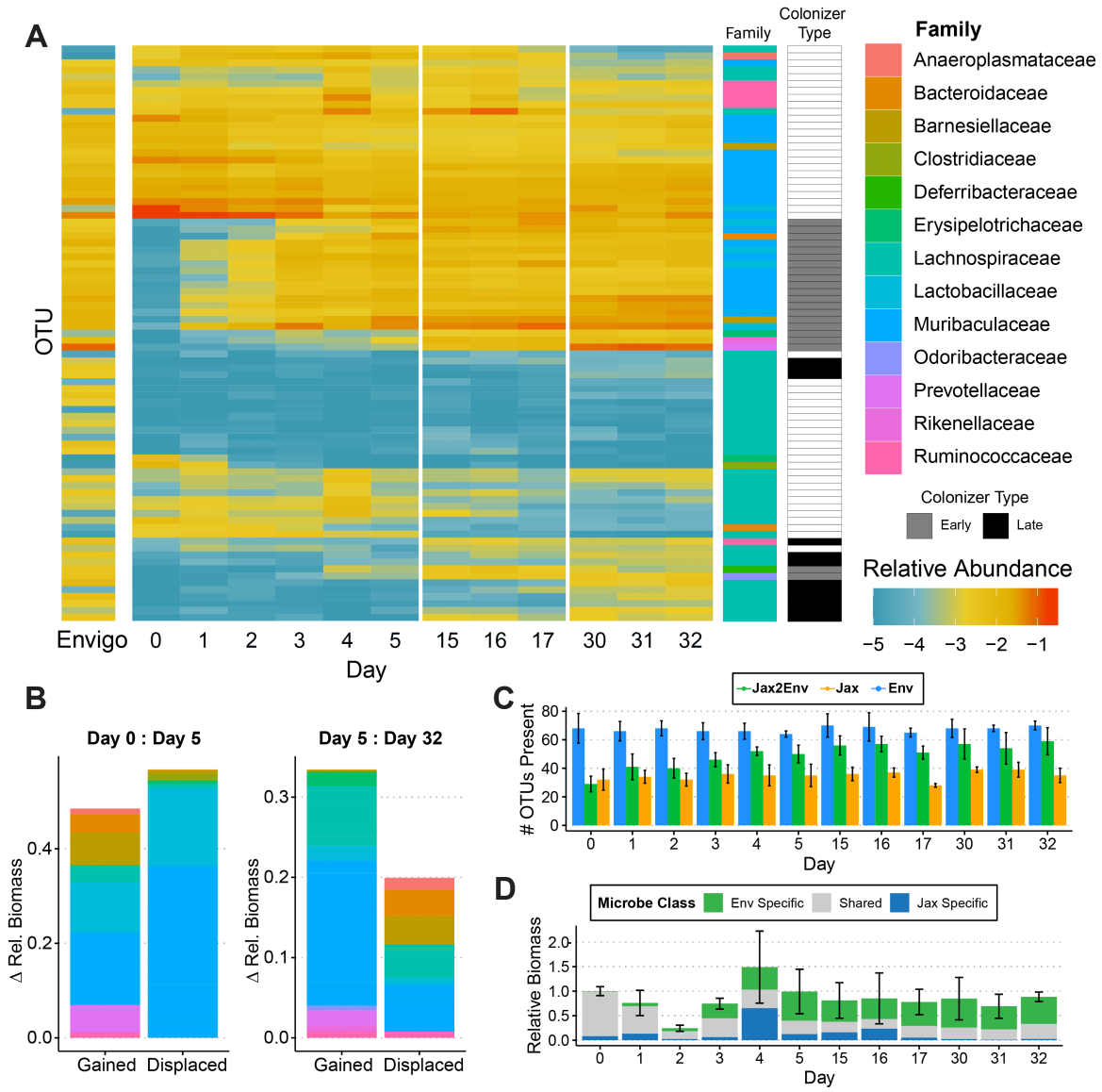

Figure 3. **The transfer of microbes by FMT occurs over short and long-time scales. (A)** Longitudinal 16S microbiome profiling of Jax2Env mice (N = 5). Detectable colonization by transferred OTUs occurs during both early (days 1-5) and late (days 15-32) sampling points. **(B)** Quantification of absolute bacterial biomass gained and lost relative to Jax mice. Biomass values are stratified by taxonomic identity comparing days 0 through 5 (left) and days 5 through 32 (right). **(C)** Number of OTUs detected over time within each mouse cohort. **(D)** Changes in bacterial biomass within feces of Jax2Env mice relative to Jax mice. Biomass is colored by whether OTUs are uniquely found in microbiomes of Envigo donors (Donor specific), uniquely found in Jackson Recipients (Recipient specific), or observed in both.

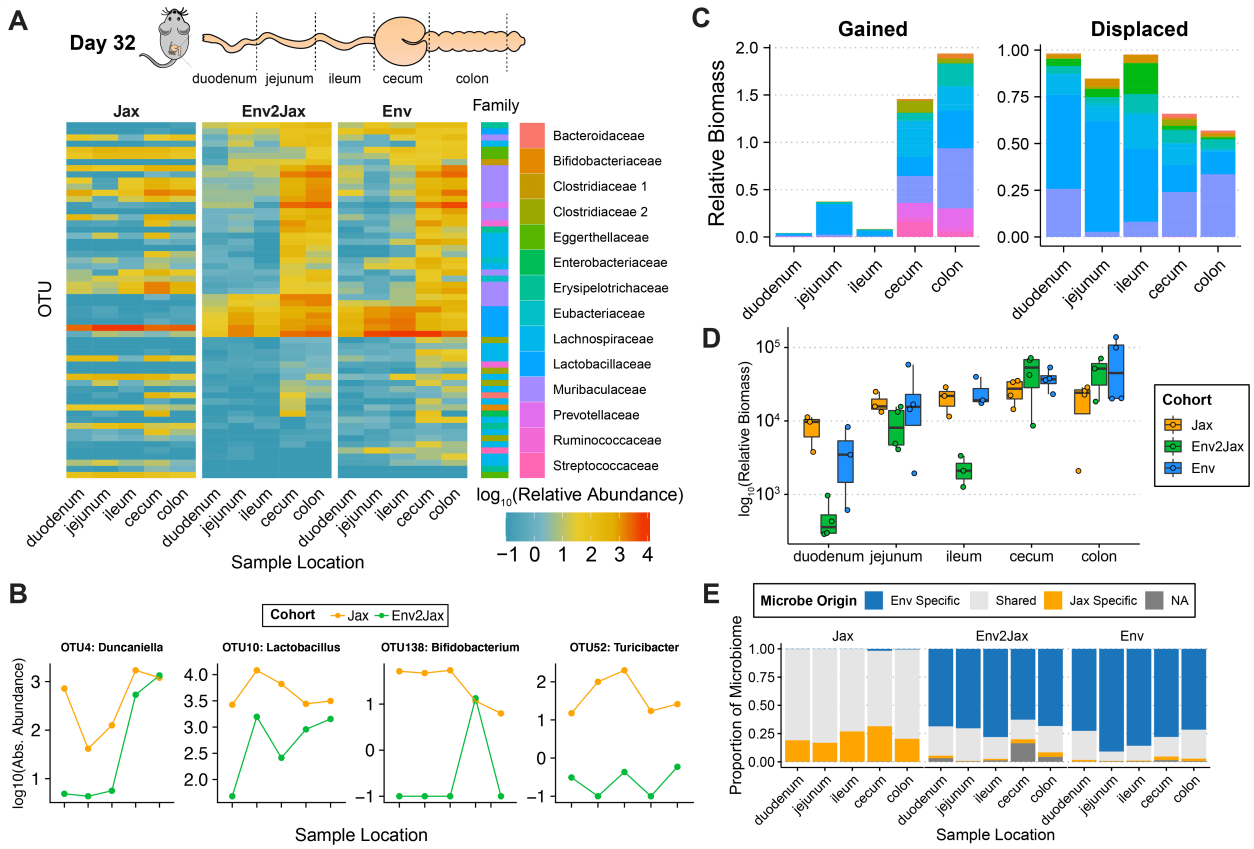

Figure 4. Microbial transplantation dynamics vary across murine gut compartments. (A) 16S profiling of luminal contents of mice cohorts after 32 days of cohousing. Rows are arranged by hierarchical clustering of cohoused Jackson cohort. **(B)** Absolute abundance of OTUs across gut compartments in Jax and Jax2Env mouse cohorts. **(C)** Quantification of absolute bacterial biomass gained (left)and lost (right) across all gut compartments stratified by taxonomic identity. Values are presented as relative to Ctrl biomass. **(D)** Proportion of bacterial biomass in each gut compartment uniquely found in Envigo donors (Donor specific), uniquely found in Jackson Recipients (Recipient specific), or observed in both. **(E)** Absolute bacterial biomass in all gut compartments across mouse cohorts.

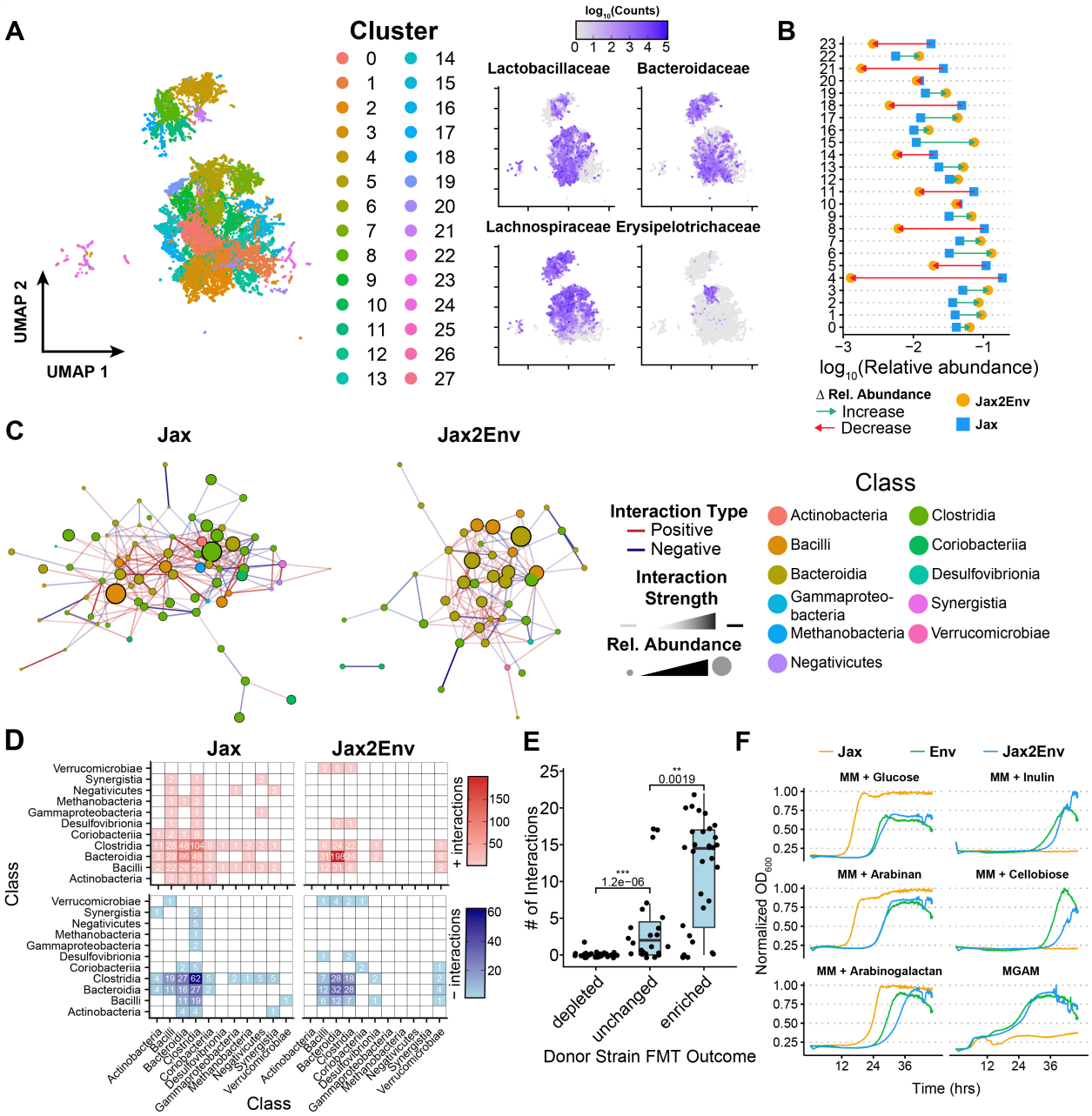

Figure 5. FMT results in dramatic restructuring of ecological interactions within populations. (A) (left) UMAP visualization of 25,942 MaPS-Seq particles from Jax, Jax2Env, and Env fecal communities. Particles are assigned community clusters based on the euclidean distance of their OTU composition. (right) 16S sequencing counts of abundant bacterial families within particles. **(B)** Change in relative abundance of particles corresponding to each of the 27 identified community clusters. Clusters are arranged bottom to top by absolute reads corresponding to each cluster. **(C)** Network visualization of significant bacterial interactions observed in Jax and Jax2Env communities. Node size indicates the relative abundance of the

OUT in the population and the opacity of the edges indicates the strength of the interaction. Red: Positive ecological interaction, Blue: Negative ecological interaction. **(D)** Number of significant (top) positive and (bottom) negative interactions detected between members of taxonomic classes found in Jax and Jax2Env microbiomes. **(E)** Number of interactions found amongst donor strains that were depleted, unchanged, or enriched in recipient (Wilcox test). Depleted: >2-fold decrease in abundance, Enriched: >2-fold increase in abundance. **(F)** OD_{600} Growth assays of fecal communities acquired from Jax, Jax2Env, and Env mice after five days of cohousing. Communities were inoculated in defined minimal media supplemented with single sources of carbohydrates (indicated).

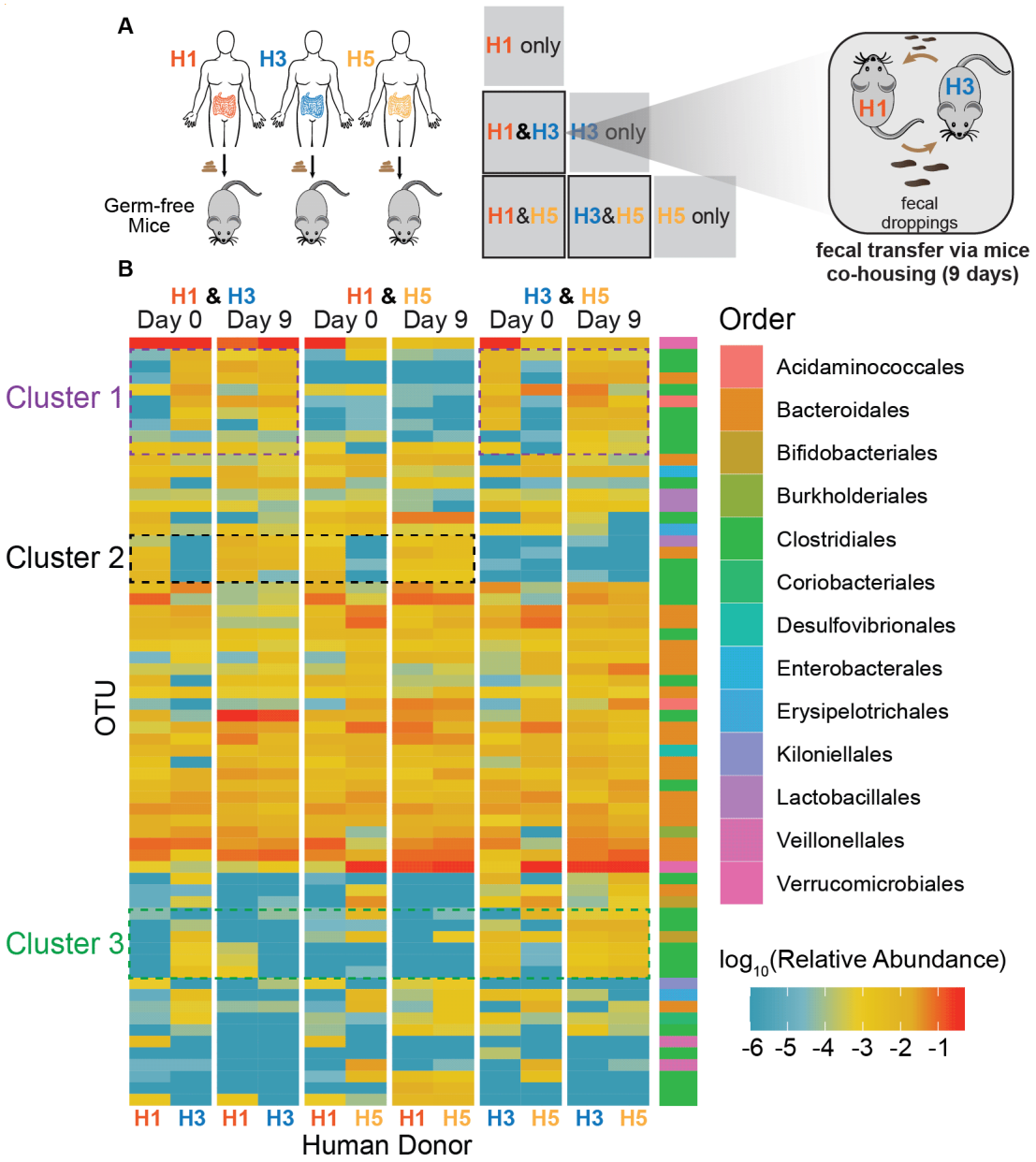

Figure 6. Humanized mouse microbiomes simulate human FMT outcomes. **(A)** Pairwise fecal microbiota (FMT) transfer model of gnotobiotic female BL57BL/6 mice harboring 'humanized' microbiomes from individuals spanning the three canonical enterotypes. **(B)** 16S profiling of mouse fecal communities following nine days of cohousing separated by pairs (N=2 per pair). Clusters 1 through 3 indicate observed microbial transfer events. Rows arranged by hierarchical clustering.

RESOURCE AVAILABILITY

Lead contact

Further information and requests for resources and reagents should be directed to and will be fulfilled by the lead contact, Harris Wang (hw2429@cumc.columbia.edu).

Materials availability

This paper does not report original materials.

Data and code availability

- Raw sequencing data is available through SRA under with accession code TBD.
- Original code and processed datasets are available through https://github.com/TBD
- Any additional information required to reanalyze the data reported in this paper is available from the lead contact upon request.

EXPERIMENTAL MODEL AND SUBJECT DETAILS

Mouse lines

C57BL6/J Mice were separately purchased from Jackson Laboratory, Taconic Biosciences, Envigo, and Charles River Laboratories.

METHOD DETAILS

Animal procedures. 6- to 8-week-old female C57BL6/J mice were obtained from different suppliers and allowed to acclimate to the animal facility for a week in cages of four mice. After one week, the bedding was exchanged between cages of mice from the same vendor to normalize their microbiota. To enable FMT by cohousing, after normalization, two of mice were transferred to a new cage along with two mice acquire from a different vendor. In control groups, all cohoused mice were from the same vendor. Mice were fed Teklad global 18% protein (2018S).

Mice feces collection and microbial DNA extraction. Fresh mouse fecal pellets were collected and kept on dry ice before being weighed and transferring to a -80°C freezer for long-term strorage. Whole pellets were suspended in 1 mL PBS and mechanically separated using an inoculating loop. Genomic DNA (gDNA) of fecal microbe were extracted using a silica bead beating-based protocol adapted from Qiagen MagAttract PowerMicrobiome DNA/RNA Kit [Qiagen 27500-4-EP], detailed fully in Ref[54]. For experiments in which absolute abundance was determined, 1 uL of saturated *Sporosarcina pasteurii* (ATCC 11859) culture was added to the sample prior to bead beating.

Luminal Content Collection. The luminal contents of mice were extracted for 16S and metagenomic sequencing. Mice were euthanized and their intestinal tracts were dissected in a sterile hood. The small intestines were separated into three sections of equal length, and their gut contents as well as those of the cecum and large intestines were extruded into 1.5 mL tubes and transferred to dry ice using forceps. Samples were weighed and processed following the microbial DNA extraction protocol described above.

16S rRNA amplicon sequencing. 16S sequencing of the V4 region for mice gut microbiota was performed using a custom library preparation and sequencing protocol with dual indexing strategy [54]. Briefly, a 20uL 16S-V4 PCR reaction was set up (1ng extracted gDNA; 1uL forward barcoded P5 primer; 1uL reverse barcoded P7 primer; 10uL NEBNext® Ultra™ II Q5® Master Mix [NEB M0544X]; SYBR Green I at 0.2x final concentration) and subjected to a quantitative amplification on a thermal cycler (98°C 30s; cycles: 98°C 10s, 55°C 20s, 65°C 60s; 65°C 5min; 4°C infinite). PCR reaction was stopped during exponential phase to avoid amplification bias (typically 13-16 cycles) and the cycling was skipped to the final extension step. Next, yielding 16S-V4 amplicon libraries were pooled based on the fluorescence increase at last cycle and subjected to gel electrophoresis. DNA bands at ~390bp were excised from gel and purified using Wizard™ SV Gel and PCR Cleanup System (Promega A9282) following the manufacturer's instructions. Purified libraries were sequenced on Illumina MiSeq platform (reagent kits: v2 300-cycles, paired-end mode) at 8 pM loading concentration with 25% PhiX spike-in (Illumina FC-110-3001). Custom sequencing primers were spiked into reagent cartridge (well 12: 16SV4_read1, well 13: 16SV4_index1, well 14: 16SV4_read2) following the manufacturer's instructions. Sequences of all primers used in library preparation and sequencing are provided in the **Supplementary Table S1**.

16S rRNA amplicon analysis and OTU clustering. Raw sequencing reads of 16SV4 amplicon were analyzed by USEARCH v11.0.667[55] (Ref.). Specifically, paired-end reads were merged using "-fastq_mergepairs" mode with default setting. Merged reads were then subjected to quality filtering using "-fastq_filter" mode with the option "-fastq_maxee 1.0 -fastq_minlen 240" to only keep reads with less than 1 expected error base and greater than 240bp. Remaining reads were deduplicated (-fastx_uniques) and clustered into OTUs (-unoise3) at 100% identity, and merged reads were then searched against OTU sequences (-otutab) to generate OTU count table. Taxonomy of OTUs were assigned using Ribosomal Database Project classifier trained with 16S rRNA training set 16.

OTU Filtering and Count Normalization. OTU count tables were normalized to relative or absolute abundance and filtered by relative abundance for downstream analyses. For experiments lacking spike-in controls, reads were normalized by relative abundance within each sample and OTUs with a relative abundance below 0.5% (averaged across biological replicates) were removed. Absolute abundance measurements were determined by normalizing relative abundance of all OTUs to spike-in OTU counts as well as the weight of the fecal pellet.

Shotgun metagenome sequencing. Library preparation of shotgun metagenome sequencing were performed using the same gDNA used for 16SV4 amplicon sequencing. Briefly, Nextera libraries were prepared following a scale-down Tn5 tagmentation-based library preparation protocol with 2ng gDNA as input[56]. Yielding libraries were sequenced on Illumina Nextseq 500/550 platform (2 x 75bp) and HiSeq platform (2 × 150bp) following the manufacturer's instructions.

Metagenome assembly and binning. Raw reads of shotgun metagenome sequencing were then processed by Cutadapt v2.1 with following parameters "--minimum-length 25:25 -u 5 -U 5 -q 15 --max-n 0 --pair-filter=any" to remove Nextera adapters and low-quality bases. To obtain metagenome-assembled genomes (MAGs) of mice gut microbiota, processed raw reads of each supplier were firstly assembled using metaSPAdes v3.11.1 with default parameters. Yielding contigs of each supplier were split into 10kb fragments to denoise assembling artifacts and then subjected to binning by MaxBin v2.2.6, MetaBAT v2.12.1, CONCOCT v1.0.0, and MyCC (no version info) with default settings. Results from different tools were further integrated and corrected by DAS Tool v.1.1.1 to generate first round of metagenome bins. Raw reads were then aligned to metagenome bins using Bowtie2 v2.3.4 in "—very-sensitive" mode and partitioned into

bins based on alignments. Next, partitioned reads of each bin were assembled separately by Unicycler v.0.4.4 with default setting to generate final MAGs. All MAGs were then evaluated for quality and contamination by Quast v4.6.3 and CheckM v1.0.13 and subsequently annotated by Prokka v1.12.

MaPS-Seq Sample Collection. Fresh fecal pellets were collected and immediately transferred to tubes containing methacarn (60% methanol, 30% chloroform, 10% acetic acid). After 24 hrs of fixation, samples were transferred to 70% ethanol and stored at 4°C until use. Samples were processed following the MaPS-Seq protocol. After fracturing and barcoding, 20-40 micron particles were isolated by size-exclusion filtering for sequencing. For each mouse, two technical replicates of approximately 10,000 particles were used for sequencing. Samples were sequenced on an Illumina NextSeq550 (2 x 250 bp)

Spatial association analysis within MaPS-Seq Particles. An empirical Bayes analysis was performed to identify spatial associations between OTUs. Briefly, OTU counts in each particle were binarized to create a matrix representing the presence or absence of each OTU in each particle. To simulate a null model of co-occurrence, we used the EcoSimR package v0.1.0 to randomly shuffle presence and absence counts and count the number of particles each OTU pair was found together for. This was performed 1000 times for each sample to generate distribution of co-occurrence frequencies for each OTU pair. We then determined where the actual co-occurrence frequency was along this distribution and calculated the Z-score. P-values were adjusted using a Bonferroni correction and an adjusted p-value < 0.05 was considered significant. Network analysis was performed in R using the packages ggraph v2.0 and igraph v1.3.1 using co-occurrence Z-scores to indicate the magnitude of relationships.

Polysaccharide Utilization Growth Assays. Fecal communities were grown in Bacteroides minimal media[57] cultures supplemented with various polysaccharides. Fecal pellets were mechanically separated in 1 mL PBS and diluted 1:10 in PBS before being inoculated in a 96-well culture for a total dilution rate of 1:400. Cultures were supplemented with 10 mg/mL of a single carbohydrate. The resulting inoculated cultures were grown over 48 hrs in a Biotek Powerwave XS plate reader (product code: B-PWXS) taking OD_{600} measurements every 15 minutes and the data was exported for analysis in R.

Ethical review. This study was approved and conducted under Columbia University Medical Center Institutional Animal Care and Use Committee (Protocol #AC-AABD4551) and complied with all relevant regulations.

Acknowledgements

We thank members of the Wang laboratory for advice and comments on the manuscript. H.H.W. acknowledges funding support from the NSF (MCB-2025515), NIH (1R01AI132403, 1R01DK118044, 1R21AI146817), ONR (N00014-18-1-2237, N00014-17-1-2353), Burroughs Wellcome Fund (1016691), Irma T. Hirschl Trust, and Schaefer Research Award. G.U. was supported by the HHMI Hanna H. Gray Postdoctoral Fellowship (GT15182). T.M. is supported by NIH Medical Scientist Training Program (T32GM007367). R.U.S. was supported by a Fannie and John Hertz Foundation Fellowship and an NSF Graduate Research Fellowship (DGE-1644869). M.R. and F.V.C. are supported by NSF Graduate Research Fellowships (DGE-1644869).

1. Lynch, S. V. & Pedersen, O. The Human Intestinal Microbiome in Health and Disease. *N. Engl. J. Med.* **375**, 2369–2379 (2016).
2. Chiu, L. *et al.* Protective Microbiota: From Localized to Long-Reaching Co-Immunity. *Front. Immunol.* **0**, (2017).
3. Martin, A. M., Sun, E. W., Rogers, G. B. & Keating, D. J. The Influence of the Gut Microbiome on Host Metabolism Through the Regulation of Gut Hormone Release. *Front. Physiol.* **0**, (2019).
4. Wernroth, M.-L. *et al.* Development of gut microbiota during the first 2 years of life. *Sci. Rep.* **12**, 9080 (2022).
5. Kim, S., Covington, A. & Pamer, E. G. The intestinal microbiota: Antibiotics, colonization resistance, and enteric pathogens. *Immunol. Rev.* **279**, 90–105 (2017).
6. Faintuch, J. & Faintuch, S. *Microbiome and Metabolome in Diagnosis, Therapy, and other Strategic Applications*. (Academic Press, 2019).
7. Bucci, V. *et al.* MDSINE: Microbial Dynamical Systems INference Engine for microbiome time-series analyses. *Genome Biol.* **17**, 121 (2016).
8. Lee, J.-Y., Tsolis, R. M. & Bäumler, A. J. The microbiome and gut homeostasis. *Science* **377**, eabp9960 (2022).
9. Olsson, L. M. *et al.* Dynamics of the normal gut microbiota: A longitudinal one-year population study in Sweden. *Cell Host Microbe* **30**, 726–739.e3 (2022).
10. Rakoff-Nahoum, S., Coyne, M. J. & Comstock, L. E. An ecological network of polysaccharide utilization among human intestinal symbionts. *Curr. Biol.* **24**, 40–49 (2014).
11. Flint, H. J., Scott, K. P., Duncan, S. H., Louis, P. & Forano, E. Microbial degradation of complex carbohydrates in the gut. *Gut Microbes* **3**, 289–306 (2012).
12. Marion, S. *et al.* Biogeography of microbial bile acid transformations along the murine gut. *J. Lipid Res.* **61**, 1450–1463 (2020).
13. Scales, B. S., Dickson, R. P. & Huffnagle, G. B. A tale of two sites: how inflammation can

reshape the microbiomes of the gut and lungs. *J. Leukoc. Biol.* **100**, 943–950 (2016).

14. Venturelli, O. S. *et al.* Deciphering microbial interactions in synthetic human gut microbiome communities. *Mol. Syst. Biol.* **14**, e8157 (2018).
15. Lozupone, C. A., Stombaugh, J. I., Gordon, J. I., Jansson, J. K. & Knight, R. Diversity, stability and resilience of the human gut microbiota. *Nature* **489**, 220–230 (2012).
16. Wilson, B. C., Vatanen, T., Cutfield, W. S. & O'Sullivan, J. M. The Super-Donor Phenomenon in Fecal Microbiota Transplantation. *Front. Cell. Infect. Microbiol.* **0**, (2019).
17. Smillie, C. S. *et al.* Strain Tracking Reveals the Determinants of Bacterial Engraftment in the Human Gut Following Fecal Microbiota Transplantation. *Cell Host Microbe* **23**, 229–240.e5 (2018).
18. Vermeire, S. *et al.* Donor Species Richness Determines Faecal Microbiota Transplantation Success in Inflammatory Bowel Disease. *J. Crohns. Colitis* **10**, 387–394 (2015).
19. The Integrative Human Microbiome Project. *Nature* **569**, 641–648 (2019).
20. Velazquez, E. M. *et al.* Endogenous Enterobacteriaceae underlie variation in susceptibility to Salmonella infection. *Nature Microbiology* **4**, 1057–1064 (2019).
21. Wolff, N. S. *et al.* Vendor effects on murine gut microbiota and its influence on lipopolysaccharide-induced lung inflammation and Gram-negative pneumonia. *Intensive Care Medicine Experimental* **8**, 1–13 (2020).
22. Ericsson, A. C. *et al.* Effects of Vendor and Genetic Background on the Composition of the Fecal Microbiota of Inbred Mice. *PLoS One* **10**, e0116704 (2015).
23. Magne, F. *et al.* The Firmicutes/Bacteroidetes Ratio: A Relevant Marker of Gut Dysbiosis in Obese Patients? *Nutrients* **12**, (2020).
24. Ley, R. E. *et al.* Obesity alters gut microbial ecology. *Proc. Natl. Acad. Sci. U. S. A.* **102**, 11070–11075 (2005).
25. Duan, R., Zhu, S., Wang, B. & Duan, L. Alterations of Gut Microbiota in Patients With Irritable Bowel Syndrome Based on 16S rRNA-Targeted Sequencing: A Systematic

Review. *Clin. Transl. Gastroenterol.* **10**, e00012 (2019).

26. Lloyd-Price, J. *et al.* Multi-omics of the gut microbial ecosystem in inflammatory bowel diseases. *Nature* **569**, 655–662 (2019).
27. Weingarden, A. *et al.* Dynamic changes in short- and long-term bacterial composition following fecal microbiota transplantation for recurrent Clostridium difficile infection. *Microbiome* **3**, 1–8 (2015).
28. Bokoliya, S. C., Dorsett, Y., Panier, H. & Zhou, Y. Procedures for Fecal Microbiota Transplantation in Murine Microbiome Studies. *Front. Cell. Infect. Microbiol.* **0**, (2021).
29. Ericsson, A. C., Personett, A. R., Turner, G., Dorfmeyer, R. A. & Franklin, C. L. Variable Colonization after Reciprocal Fecal Microbiota Transfer between Mice with Low and High Richness Microbiota. *Front. Microbiol.* **8**, 196 (2017).
30. Seedorf, H. *et al.* Bacteria from Diverse Habitats Colonize and Compete in the Mouse Gut. *Cell* **159**, 253–266 (2014).
31. Li, W. *et al.* A Cross-Scale Neutral Theory Approach to the Influence of Obesity on Community Assembly of Human Gut Microbiome. *Front. Microbiol.* **0**, (2018).
32. Sloan, W. T. *et al.* Quantifying the roles of immigration and chance in shaping prokaryote community structure. *Environ. Microbiol.* **8**, 732–740 (2006).
33. Podlesny, D. *et al.* Identification of clinical and ecological determinants of strain engraftment after fecal microbiota transplantation using metagenomics. *Cron. Med.* **3**, (2022).
34. Donaldson, G. P., Lee, S. M. & Mazmanian, S. K. Gut biogeography of the bacterial microbiota. *Nat. Rev. Microbiol.* **14**, 20–32 (2015).
35. Tropini, C., Earle, K. A., Huang, K. C. & Sonnenburg, J. L. The Gut Microbiome: Connecting Spatial Organization to Function. *Cell Host Microbe* **21**, 433–442 (2017).
36. Turnbaugh, P. J. *et al.* The effect of diet on the human gut microbiome: a metagenomic analysis in humanized gnotobiotic mice. *Sci. Transl. Med.* **1**, 6ra14 (2009).

37. Zmora, N. *et al.* Personalized Gut Mucosal Colonization Resistance to Empiric Probiotics Is Associated with Unique Host and Microbiome Features. *Cell* **174**, 1388–1405.e21 (2018).
38. Hu, J. *et al.* Gut microbiota-mediated secondary bile acids regulate dendritic cells to attenuate autoimmune uveitis through TGR5 signaling. *Cell Rep.* **36**, (2021).
39. Ridlon, J. M., Wolf, P. G. & Gaskins, H. R. Taurocholic acid metabolism by gut microbes and colon cancer. *Gut Microbes* **7**, 201–215 (2016).
40. Hibbing, M. E., Fuqua, C., Parsek, M. R. & Peterson, S. B. Bacterial competition: surviving and thriving in the microbial jungle. *Nat. Rev. Microbiol.* **8**, 15–25 (2009).
41. Sheth, R. U. *et al.* Spatial metagenomic characterization of microbial biogeography in the gut. *Nat. Biotechnol.* **37**, 877–883 (2019).
42. Gotelli, N. J. & Ulrich, W. The empirical Bayes approach as a tool to identify non-random species associations. *Oecologia* **162**, 463–477 (2010).
43. Kearney, S. M., Gibbons, S. M., Erdman, S. E. & Alm, E. J. Orthogonal Dietary Niche Enables Reversible Engraftment of a Gut Bacterial Commensal. *Cell Rep.* **24**, 1842–1851 (2018).
44. Shepherd, E. S., DeLoache, W. C., Pruss, K. M., Whitaker, W. R. & Sonnenburg, J. L. An exclusive metabolic niche enables strain engraftment in the gut microbiota. *Nature* **557**, (2018).
45. Arumugam, M. *et al.* Enterotypes of the human gut microbiome. *Nature* **473**, 174–180 (2011).
46. Park, J. C. & Im, S.-H. Of men in mice: the development and application of a humanized gnotobiotic mouse model for microbiome therapeutics. *Exp. Mol. Med.* **52**, 1383–1396 (2020).
47. Levy, R. *et al.* Longitudinal analysis reveals transition barriers between dominant ecological states in the gut microbiome. *Proc. Natl. Acad. Sci. U. S. A.* **117**, 13839–13845 (2020).
48. Jones, B. V., Begley, M., Hill, C., Gahan, C. G. M. & Marchesi, J. R. Functional and

comparative metagenomic analysis of bile salt hydrolase activity in the human gut microbiome. *Proc. Natl. Acad. Sci. U. S. A.* **105**, 13580–13585 (2008).

49. Theriot, C. M., Bowman, A. A. & Young, V. B. Antibiotic-Induced Alterations of the Gut Microbiota Alter Secondary Bile Acid Production and Allow for Clostridium difficile Spore Germination and Outgrowth in the Large Intestine. *mSphere* **1**, (2016).
50. Rowland, I. *et al.* Gut microbiota functions: metabolism of nutrients and other food components. *Eur. J. Nutr.* **57**, 1–24 (2018).
51. Frazier, K. & Chang, E. B. Intersection of the Gut Microbiome and Circadian Rhythms in Metabolism. *Trends Endocrinol. Metab.* **31**, 25–36 (2020).
52. Liao, J. *et al.* The importance of neutral and niche processes for bacterial community assembly differs between habitat generalists and specialists. *FEMS Microbiol. Ecol.* **92**, fiw174 (2016).
53. Button, J. E. *et al.* Dosing a synbiotic of human milk oligosaccharides and B. infantis leads to reversible engraftment in healthy adult microbiomes without antibiotics. *Cell Host Microbe* **30**, 712–725.e7 (2022).
54. Ji, B. W. *et al.* Quantifying spatiotemporal variability and noise in absolute microbiota abundances using replicate sampling. *Nat. Methods* **16**, 731–736 (2019).
55. Edgar, R. C. Search and clustering orders of magnitude faster than BLAST. *Bioinformatics* **26**, 2460–2461 (2010).
56. Baym, M. *et al.* Inexpensive Multiplexed Library Preparation for Megabase-Sized Genomes. *PLoS One* **10**, e0128036 (2015).
57. Bacic, M. K. & Smith, C. J. Laboratory maintenance and cultivation of bacteroides species. *Curr. Protoc. Microbiol.* **Chapter 13**, Unit 13C.1 (2008).